KSME

Springer

Journal of Mechanical Science and Technology 37 (9) 2023

Original Article
DOI 10.1007/s12206-023-0839-1

Keywords:
· Heat transfer characteristics
· Pulsating heat pipe
· Thermal management
· Computational fluid dynamics
· Heat and mass transfer

Correspondence to:
Yongseok Jeon
ysjeon@kmou.ac.kr

Citation:
Jung, J., Jeon, Y. (2023). Numerical study on the heat transfer characteristics of three-dimensional pulsating heat pipe. Journal of Mechanical Science and Technology 37 (9) (2023) 4869~4876. http://doi.org/10.1007/s12206-023-0839-1

Received September 22nd, 2022
Revised April 17th, 2023
Accepted June 3rd, 2023

† Recommended by Editor Tong Seop Kim

Numerical study on the heat transfer characteristics of three-dimensional pulsating heat pipe

Jongmin Jung[1] and Yongseok Jeon[2]

[1]Graduate School of Refrigeration and Air Conditioning Engineering, Korea Maritime and Ocean University, Busan 49112, Korea, [2]Department of Mechanical Engineering, Korea Maritime and Ocean University, Busan 49112, Korea

Abstract Existing pulsating heat pipes (PHPs) have a closed loop on a two-dimensional (2D) plane, leading to a structural limit in heat transfer performance. This study solves the limitations of these existing PHPs by substituting a specific three-dimensional (3D) structure PHP. The numerical model (having a 2D structure PHP) was validated with the experiment, which shows the maximum error of 8.5 % in the results. Results show that additional flow occurred due to the 3D structure of the PHP, which enables improved heat transfer. Under uniform heating conditions, the thermal resistance and the temperature of the evaporator decreased by up to 14.7 % and 6.7 °C, respectively. Finally, the heat transfer performance was compared for the entire 3D structure PHP under uniform and non-uniform heating conditions. The non-uniform heating conditions of the PHP increased the thermal resistance and temperature of the evaporator under low heating rates while decreased them under high heating rates.

1. Introduction

With the recent industrial developments, electronic equipment is being miniaturized, battery capacity and energy density are increasing, and the amount of heat generated per unit area is continuously increasing. Therefore, thermal management is becoming an important factor in determining the service life, performance, and stability of these devices. Among various methods for thermal management of electronic equipment or batteries, extensive research has been conducted on heat pipes using fluid to effectively transfer or manage heat by using the latent heat of evaporation. In particular, a pulsating heat pipe (PHP), in which the tube is composed of several loops on a two-dimensional plane, has no wick structure; therefore, the structure is simple, and the design can be applied flexibly, unlike the conventional heat pipe structure. In addition, there is an advantage in that the thermal properties are superior to those of the conventional heat pipe due to heat transfer by pulsating generated due to phase change and internal pressure imbalance [1].

PHP has been studied extensively as a heat transfer medium [2]. Youn and Kim [3] analyzed the thermal characteristics of silicon-based micro-PHP according to filling ratio, inclination angle, and thermal load. As a result, the heat transfer rate of PHP is reported to be approximately 1.5 times higher than that of copper. Jang et al. [4] analyzed the thermal characteristics according to the asymmetry and aspect ratio of the PHP flow path and proposed an optimal flow path design according to the thermal load. Patel et al. [5] analyzed PHP performance using 1) pure water, ethanol, methanol, and acetone, 2) mixtures of water with ethanol, methanol, acetone, and 3) water-based surfactant solutions. In addition, some studies using different types of fluids [6, 7] and nanofluids as working fluids have been conducted [8, 9]. Combining the results of previous studies, the heat transfer performance of PHP is influenced by the operating conditions (working fluid, filling ratio, and heat load) [10], as well as design variables (inner diameter, length, asymmetry, number of turns, and inclination angle) [11, 12].

A large amount of heat entering the heat pipes evaporates the liquid phase in the evaporator,

leading to a dry-out in which the liquid phase disappears on the heating surface, thereby significantly reducing the heat transfer rate. Numerous studies are being conducted to address these problems. Furthermore, several numerical studies using experiments and computational fluid dynamics (CFD) are being conducted to investigate the complex phase change flow phenomenon inside PHPs. However, heat pipe analysis deals with an ideal flow accompanied by a phase change, which requires considerable computational power because phase change occurs continuously through multiple loops. As existing numerical studies on PHPs has limitations in numerically predicting numerous phase change processes, many studies attempted to perform the analysis using the 2D model [13, 14] or treating the physical properties of the working fluid as a constant value [14-16]. Kang et al. [13] used a 2D numerical model to analyze a single loop PHP with separating walls located at the flow channel using variable properties of the working fluid. Wang et al. [14] also used a 2D numerical model to analyze the single loop PHP with different diameter ratios. Wang et al. [15, 16] analyzed a single loop PHP with a 3D numerical model using CTAC solution as the working fluid at different initial pressures and wettability levels. Wang et al. [15] used a 3D numerical model to analyze a single loop PHP by varying the surfactant and working fluid mixing ratios. The same authors [16] analyzed the same numerical model under various wettability settings. Most experimental studies focused on optimizing the filling ratio and shape according to the heating rate applied to PHP within a two-dimensional structure, or analyzing flow characteristics. PHP can be manufactured in a flat plate type, and for thermal management in batteries or electronic equipment, manufacturing it in a three-dimensional (3D) structure improves space utilization and reduces the temperature deviation between PHPs. When a specific PHP receives a high amount of heat under a non-uniform heating condition, dry-out can be delayed by the flow of the working fluid inside the surrounding PHP. Despite these advantages, prior studies related to the three-dimensional structure of PHP included Han et al. [17] analyzing the flow characteristics by connecting the condenser and the evaporator using four glass tubes, reporting that a lower filling ratio facilitated dry-out. Chu et al. [18] changed the flow path close to 3D by configuring the evaporator of PHP in the form of a spiral coil, while Qu et al. [19] analyzed the heat transfer characteristics by bending the evaporator of PHP and constructing it three-dimensionally. However, 3D structure PHP-related studies mentioned above only attempted to change the flow path of the evaporator by configuring the contact part to be three-dimensional. No studies on 3D structure PHP in which separate flat-type PHPs are connected three-dimensionally have been conducted. Moreover, most PHP research focus on the thermal properties of the working fluid, operating conditions, and geometric parameters such as the diameter, number of turns, and length ratio of the evaporator and condenser. Therefore, this study aims to compare the heat transfer characteristics of 3D structure PHP numerically with those of 2D structure PHP and review the applicability of 3D structure PHP as a thermal management system for electronic equipment or battery packs in the future.

In this study, the heat transfer characteristics under different heating conditions were analyzed numerically by connecting the upper and lower parts of five single-loop PHPs to construct a 3D structure of PHPs. This study used a 3D model to minimize the errors of experimental and numerical analysis, and numerical analysis was performed considering the change in the physical properties of the working fluid according to temperature and pressure. Finally, the heat transfer characteristics of a PHP with a three-dimensional structure under different heating conditions are compared with PHP with a two-dimensional structure to provide basic design data for the novel 3D PHP.

2. Numerical model

2.1 PHP model

In this study, numerical analysis was performed using a commercial program, ANSYS Fluent, to model a PHP. When a PHP starts to work with a certain amount of heat applied, the internal flow pattern consists mainly of a liquid slug/vapor plug type flow pattern. Among the multiphase models, the volume of fluid (VOF) is a multiphase flow model that uses a surface tracking technique applied in a fixed mesh system to analyze the interface according to the interaction between each fluid. Therefore, the VOF model is believed to be a multiphase model suitable for analyzing PHP, and in this study, the analysis has been conducted using the VOF model. In the VOF model, when an interface between phases exists in the mesh, the ratio of each phase is expressed as a volume fraction. This study used two phases, a liquid and a vapor phase, which were α_l and α_v, respectively, and the sum of volume fraction in each analytical mesh was 1. It is calculated as α_v = 0 when only the liquid phase exists in the analytical mesh, and α_v = 1 when only the vapor phase exists. In this study, to consider the compressibility of the vapor phase and increase the stability of the analysis, the vapor and liquid phases were used as the primary and secondary phases, respectively. The governing equations [20] for continuity, momentum and energy are given below.

The continuity equations used for interfacial tracking are expressed as follows:

$$\frac{1}{\rho_v}\left[\frac{\partial}{\partial t}(\alpha_v\rho_v)+\nabla\cdot(\alpha_v\rho_v\vec{v}_v)=\dot{m}_{vl}-\dot{m}_{lv}\right] \quad (1)$$

$$\frac{1}{\rho_l}\left[\frac{\partial}{\partial t}(\alpha_l\rho_l)+\nabla\cdot(\alpha_l\rho_l\vec{v}_l)=\dot{m}_{lv}-\dot{m}_{vl}\right] \quad (2)$$

where $\dot{m}_{vl}$ denotes the mass transfer amount from the vapor phase to the liquid phase, and $\dot{m}_{lv}$ denotes the mass transfer amount from the liquid phase to the vapor phase. $\dot{m}_{vl}$ and $\dot{m}_{lv}$ are expressed as follows:

$$\dot{m}_{lv} = \beta_e \alpha_l \rho_l \frac{(T_l - T_{sat})}{T_{sat}} \quad (3)$$

$$\dot{m}_{vl} = \beta_c \alpha_v \rho_v \frac{(T_{sat} - T_v)}{T_{sat}} \quad (4)$$

where T_{sat} denotes the saturation temperature of the working fluid, T_l denotes the liquid-phase temperature, and T_v denotes the vapor-phase temperature. The LEE model [21] was used that was proposed by LEE for the phase change model, with β_e and β_c as time relaxation coefficients for evaporation and condensation processes, which were set as 0.1 and 6 s^{-1} [13], respectively, for the analysis.

The momentum and energy equations are expressed as follows:

$$\frac{\partial}{\partial t}(\rho \vec{v}) + \nabla \cdot (\rho \vec{v}\vec{v}) = -\nabla P + \nabla \cdot \left[\mu\left(\nabla \vec{v} + \nabla \vec{v}^T\right)\right] \rho \vec{g} + \vec{F} \quad (5)$$

$$\frac{\partial}{\partial t}(\rho E) + \nabla \cdot \left(\vec{v}(\rho E + p)\right) = \nabla \cdot \left(k_{eff} \nabla T\right) + S_h \quad (6)$$

Density and viscosity in the momentum equation were calculated as variables for the volume average within the mesh. A continuous surface force (CSF) model was used for the surface tension, which is an important variable in PHP analysis, mainly dealing with liquid slug/vapor plug flow. In the energy equation, energy (E) and temperature (T) were assumed to be variables for the mass average.

2.2 Numerical model validation

The numerical model validation was conducted with the same size and conditions as in the study conducted by Saha et al. [22]. The heat pipe with an inner diameter of 4 mm and a total length of 150 mm used for model verification is shown in Fig. 1. The lengths of the condenser, adiabatic section, and evaporator are 30, 60, and 60 mm, respectively. Saha et al.'s [22] employed quartz glass as the material in their study. In this study, only the fluid part was modeled, and the solid part was omitted. A shell conduction conditions were applied to all walls, using the same thickness and thermal conductivity as mentioned in Saha et al.'s [22] study. The meshes in the independence test for the four different grids were generated using ANSYS Fluent Meshing. Fig. 2 illustrates the cross-section of the generated grids. The meshes have 46113, 37572, 30309, and 25053 grids generated by polyhedral mesh with 5 layers. The grid independence test was performed under two heat input conditions of 35.77 and 55.8 W. Fig. 3 shows the thermal resistance, internal pressure, and error percentage for different heat inputs. The change in thermal resistance and internal pressure corresponding to a change in the grid number is as small as 7 % at most. To reduce errors that may occur under conditions other than the mesh independence test, and considering the computational time of the numerical analysis, 30309 grids were used in the present numerical simulation.

Table 1. Working fluid properties.

Phase	Property	Content	
	Saturation temperature	$T_{sat} = f(p)$	p : Local pressure T : Local temperature
	Surface tension	$\sigma = f(T)$	
Liquid-phase (water-liquid)	Density	$\rho_l = f(T)$	
	Viscosity	$\mu_l = f(T)$	
Vapor-phase (water-vapor)	Density	$\rho_v = P / RT$	
	Viscosity	μ_v = constant	

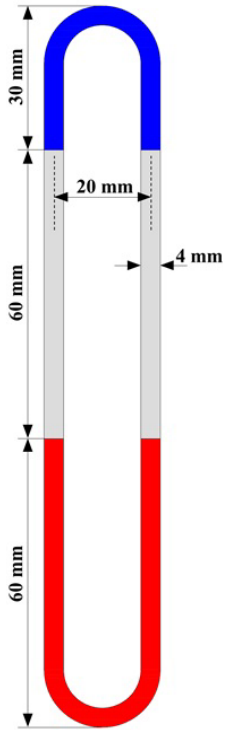

Fig. 1. Single loop pulsating heat pipe (2D structure PHP).

The heating rates of the evaporator were 35.77, 55.8, 86.62, and 97.11 W, and the temperature of the condenser was 25 °C. The filling ratio of the heat pipe was 50 %, and the working fluid was water. To apply the temperature and/or pressure dependent variable physical properties of the working fluid to the analysis, each property value of water-liquid and water-vapor was applied in the form of polynomials by curve fitting in the operating temperature range. Because the internal pressure changes according to the heating rate in a PHP, the saturation temperature of the working fluid was set as a function of the pressure, and the surface tension was set as a function of temperature. Water-vapor was set as an ideal gas to consider compressibility, and the viscosity was set as a constant value because it only slightly varies with temperature. The density and viscosity of water-liquid were set as a function of temperature. Table 1 lists the physical properties of each phase. The latent heat of evaporation was set as the latent heat of evapo-

Table 2. Boundary conditions of 2D structure PHP.

Part	Boundary conditions	Value
Evaporator	Constant heat input	35.77 W, 55.8 W, 86.62 W, 97.11 W
Adiabatic section	Adiabatic	Adiabatic
Condenser	Constant temperature	25 °C

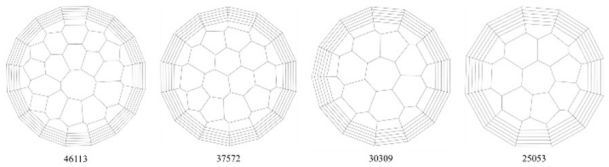

Fig. 2. Cross section of 2D structure PHP mesh under different grid numbers.

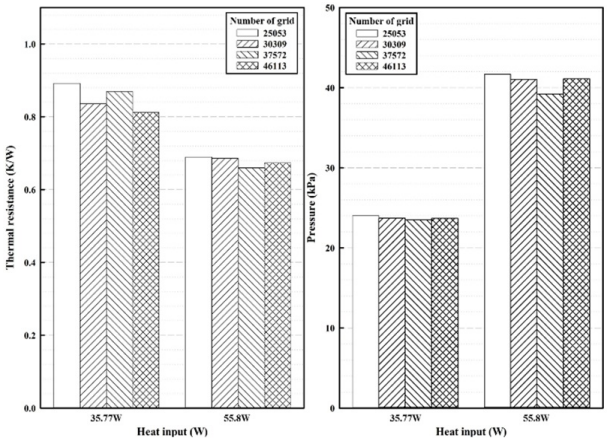

(a) (b)

Fig. 3. Grid independence test: (a) thermal resistance; (b) internal pressure.

ration of water at 30 °C. The initial conditions were at a temperature of 25 °C and a pressure of 4247 Pa. The saturation temperature of water was 30 °C at 4247 Pa. Table 2 shows the boundary conditions, and no-slip wall condition is used on all the walls. The internal flow of a PHP undergoes continuous changes in operating conditions and exhibits complex flow patterns. In the study by Vo et al. [1], the internal flow of PHP was identified as turbulent through experiments, and the k-epsilon was used for numerical analysis. Similarly, other numerical studies have also used the k-epsilon model [14-16]. Therefore, in this study, the k-epsilon model was employed for the analysis. Table 3 lists the setup of the Fluent Solver and the discretization method used for the analysis. The thermal resistance was obtained for the performance of the heat pipe by using Eq. (7).

$$R_{th} = \frac{T_E - T_C}{Q_{input}} \tag{7}$$

where T_E denotes the temperature of the evaporator, T_C denotes the temperature of the condenser, and Q_{input} denotes the heating rate. Fig. 4 shows the thermal resistance of the experiment and the numerical analysis. The error between the experimental and the numerical analysis was up to 8.5 % and the average was ±3.8 %. It indicates that the experimental and numerical analytical results are quite similar.

Table 3. Numerical simulation setting.

Items	Content	Items	Content
Model	3D, transient	Time step size	0.001 s
Surface tension	Continuum surface force (CSF)	Multiphase model	VOF explicit, Implicit body force
Viscous	k-epsilon	Pressure-velocity coupling	SIMPLE
Pressure interpolation	PRESTO	Momentum and energy	Second-order upwind
Volume fraction	Compressive	Contact angle	30°

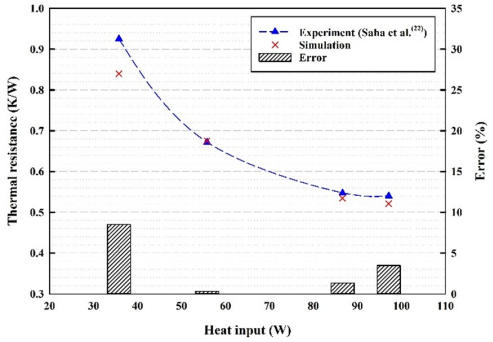

Fig. 4. Thermal resistance compares experiment and simulation.

2.3 3D PHP model

Fig. 5 shows the 3D structure PHP model used in this study, where five heat pipes identical to the verified model above in Sec. 2.2, were arranged at intervals of 20 mm, with the upper and lower parts connected by a tube with the same inner diameter. The mesh used in the 3D structure PHP was generated with the same size, shape, and boundary layers of the grid as that of the verified model. It consists of 161167 cells and 477343 nodes. The temperature of the condenser was set at 25 °C. The analysis was performed by considering two cases according to the amount of heat applied to the evaporator. In case 1, the analysis was conducted by applying uniform heating at 40, 60, 80, and 100 W to the entire heat pipe. In case 2, the analysis was conducted under the condition of heating the central heat pipe more than the surrounding heat pipes, assuming a case in which several heating elements were stacked to increase the heating rate in the center. Table 4 lists the heating conditions for each case. The 3D structure PHP analysis was conducted using the same solver settings as the 2D structure PHP analysis, as well as the discretization method and the physical properties of the working fluid.

Table 4. Simulation heat input condition.

Items	PHP 1	PHP 2	PHP 3	PHP 4	PHP 5
Case 1	40 W, 60 W, 80 W, 100 W apply the same amount of heat input to each PHP				
Case 2	60 W	80 W	100 W	80 W	60 W

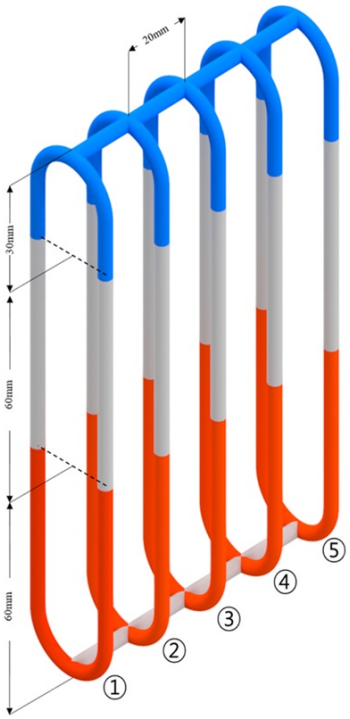

Fig. 5. Schematic of the 3D structure PHP model.

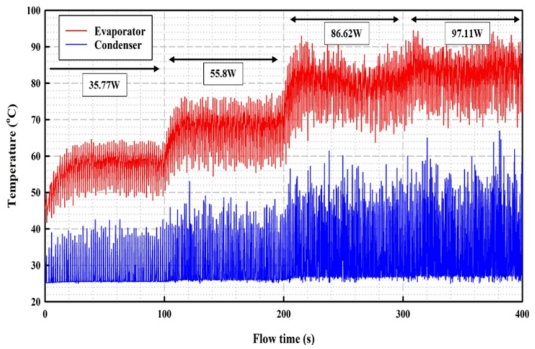

Fig. 6. Evaporator and condenser temperature at 2D structure PHP.

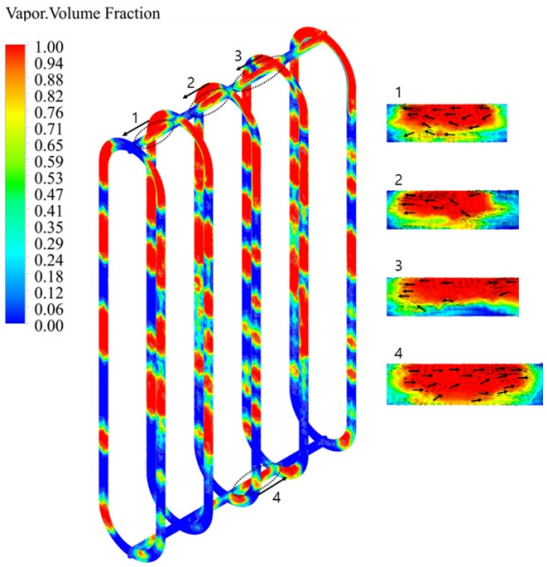

Fig. 7. 3D structure PHP vapor volume fraction.

3. Results and discussion

Fig. 6 shows the respective temperatures of the evaporator and condenser of the 2D structure PHP over time. Although the temperature changed significantly depending on the flow characteristics, the average temperature was maintained at a constant heating rate. As the heating rate increased, the temperature of the condenser and the evaporating part increased. The temperature of the evaporator increased up to 90 °C when heated at 97.11 W. Heat pipes are widely used for the thermal management of batteries and electronic equipment where the evaporator of the heat pipe is in direct or indirect contact with the device to remove heat. Therefore, the temperature of the equipment is higher than or equal to the temperature of the evaporator, and such an increase in the temperature of the evaporator causes malfunction and failure of the equipment. Therefore, the heat generated in the evaporator must be quickly transferred to the condensing unit to maintain a low temperature in the evaporator. In the 3D structure PHP used in this study, additional flow occurred compared to 2D structure PHP through the pipes connecting the evaporator and condenser at the top and bottom, respectively.

Fig. 7 shows the internal volume fraction contour and flow direction vector of the upper and lower connecting pipes during 3D PHP operation. The red and blue colors represent the vapor and liquid phases, respectively, and the arrows represent the movement direction of the vapor phase. The heat was uniformly applied to each heat pipe. The heat transfer and the flow characteristics according to the heating rate were analyzed. Liquid slug/vapor plug flow was the main flow in each heat pipe, similar to the 2D structure PHP. Unlike in 2D PHP, additional flow occurred in the upper and lower connecting pipes. As a result of analyzing the flow direction through the vector, the flow mainly occurred in the direction from PHP 5 to PHP 1 in the upper connecting pipe, and from PHP 1 to PHP 5 in the lower connecting pipe. In other words, the flow circulated as a whole, and heat is transferred in a three-dimensional direction.

Fig. 8 shows the flow velocity in the axial direction of the connecting pipe to analyze the three-dimensional flow characteristics according to the heating rate. As confirmed by the axial flow-direction vector earlier, the flow directions of the evaporator and condenser were opposite to each other. The flow from

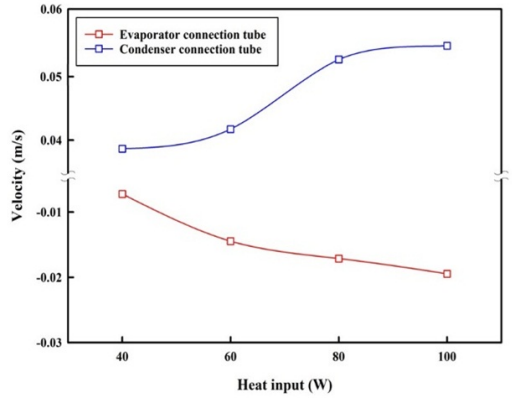

Fig. 8. Axial flow velocity at connection tube.

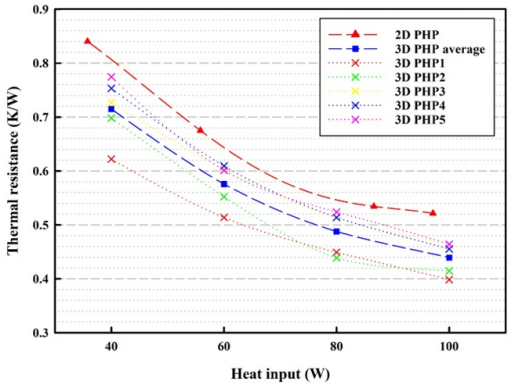

Fig. 10. Comparison of thermal resistance 2D structure PHP and 3D structure PHP.

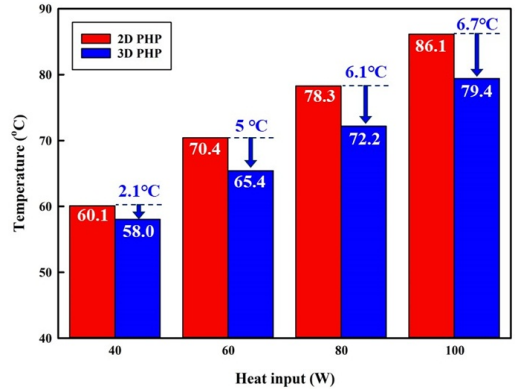

Fig. 9. Comparison of evaporator temperature 2D structure PHP and 3D structure PHP.

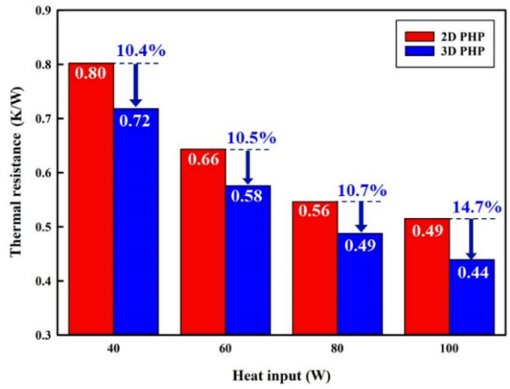

Fig. 11. Comparison of thermal resistance of the 2D and 3D PHPs at the same heat input condition.

PHP 5 to PHP 1 was expressed as a positive number, and the flow in the opposite direction was expressed as a negative number. It can be confirmed that an overall circulating flow occurred and that the velocity in the 3D connecting pipes increased as the heating rate increased in both the evaporator and the condenser connecting pipes. In other words, the effect of the three-dimensional connection on the heat transfer in PHP is increased with an increase in the heating rate.

Fig. 9 shows the evaporator temperature of 2D structure PHP and 3D structure PHP according to the heating rate. The 3D structure PHP evaporator's temperature represented the average value of the five PHP evaporator temperatures. Overall, the evaporator temperature increased with an increase in the heating rate, but the temperature change following the increase in the heating rate from 40 W to 100 W was 21.4 °C and 26 °C in 3D structure PHP and 2D structure PHP, respectively, and the temperature change was smaller for 3D structure PHP. With an increase in the heating rate, the amount of decrease in the evaporator temperature increased, which may have been due to the effect of the increase in the three-dimensional internal flow rate as described in Fig. 9. Under 40, 60, 80, and 100 W heating conditions, the temperature in the 3D structure PHP decreased by 2.1, 5, 6, and 6.7 °C, respectively, compared to the temperature in the 2D structure PHP. Therefore, the 3D structure PHP can maintain a lower evaporator temperature.

Fig. 10 shows the thermal resistance of each loop of 2D structure PHP and 3D structure PHP according to the heating rate. The thermal resistance was found to be lower in 3D structure PHP compared to 2D structure PHP due to the decrease in the evaporator temperature. The thermal resistance of 3D structure PHP was calculated similarly to the thermal resistance of 2D structure PHP. The thermal resistance of each 3D structure PHP was slightly different depending on the flow direction of the working fluid in the upper and lower connecting pipes. As shown in Figs. 6 and 7, the flow moves in one direction in the connecting pipe, and in the connecting pipe to the evaporator, the direction of flow is from PHP 1 to PHP 5. Therefore, the thermal resistance increases sequentially from PHP 1 to PHP 5. Even in PHPs 4 and 5, the thermal resistance is highest, but it was lower than that of the conventional 2D structure PHP. The average thermal resistance of 3D structure PHP was found to be reduced compared to that of 2D structure PHP. Fig. 11 shows the comparison of the average thermal resistance between the 2D and 3D structure PHPs considering the same heating rate. Similar to the temperature of the evaporator, the decrease in thermal resistance increased as the heating rate increased, and the thermal resistance was found to be decreased up to 14.7 %

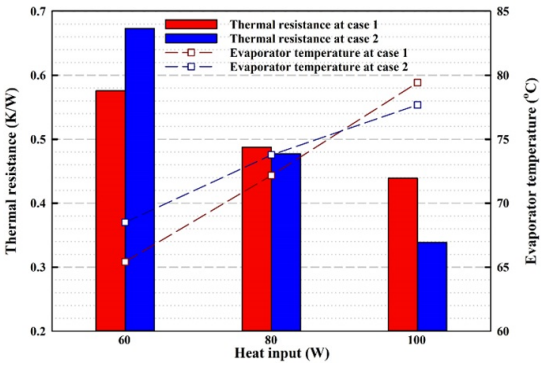

Fig. 12. Comparison of thermal resistance and evaporator temperature between cases 1 and 2.

under the 100 W heating condition.

In case 1, the analysis was conducted considering a uniform heating condition in each 3D structure PHP. In case 2, the analysis was conducted considering a non-uniform heating condition with more heat concentrated in the center as in the actual system. Fig. 12 shows the thermal resistance of each PHP under the following heating condition: evaporator temperature at 60 W for PHPs 1 and 5, 80 W for PHPs 2 and 4, and 100 W for PHP 3. The figure also expresses the results of case 1 under a uniform heating condition. The thermal resistance and the evaporator temperature in case 2 were expressed as the average values of PHPs 1 and 5, and PHPs 2 and 4, to which the same amount of heat was applied. Under the 60 W heating condition of PHPs 1 and 5 in case 2, the amount of heating was lower than that of the surrounding PHP; therefore, the heat entered through the connection pipe, increasing the evaporator temperature and thermal resistance. On the contrary, in case 2, as the heating rate was higher in PHP 3 under the 100 W heating condition than that of the surrounding PHP, the heat was transferred to the surrounding PHP through the connection pipe. Furthermore, it was compared with the 100 W heating condition of case 1; the evaporator temperature and thermal resistance were found to be decreased. In the three-dimensionally connected structure, the thermal resistance of the central part and the evaporator temperature could be reduced under the non-uniform heating condition with a large amount of heat concentrated in the center. Therefore, 3D structure PHP is expected to reduce the thermal bottleneck in the center of a structure in which heating elements are stacked similarly to a battery with the three-dimensional flow and delay dry-out in PHP.

4. Conclusions

This study conducted a numerical analysis of a new 3D structure PHP model. Prior to this numerical analysis, the numerical model was verified through the analysis of 2D structure PHP. The numerical analysis results of the 2D structure PHP were obtained with an average error of 3.8 % compared to that of the experimental results. Furthermore, the verified model was used to analyze the heat transfer characteristics in the 3D structure PHP. The new 3D structure PHP used in this study was constructed by connecting five 2D structure PHPs with an interval of 20 mm in the orthogonal direction of their plane. The heat transfer performance of the 3D structure PHP was compared with that of the 2D structure PHP, indicating that the thermal resistance and evaporator temperature decreased. The 3D structure PHP is capable of three-dimensional heat transfer by generating an additional flow through the upper and lower connecting pipes of the PHPs. Numerical analysis was carried out in two cases of uniform and non-uniform heat input conditions.

1) In a uniform heating condition of the PHP, the numerical analysis was conducted at 40, 60, 80, and 100 W. Compared to the 2D structure PHP, the evaporator temperature and thermal resistance were reduced through the additional loop in the 3D structure PHP. In addition, an increase in the heating rate increased the flow inside the 3D structure PHP. The decrease in the evaporator temperature was up to 6.7 °C, and the thermal resistance of the 3D structure PHP also decreased by up to 14.7 % compared to that of the 2D structure PHP.

2) In a non-uniform heating condition of the PHP, the numerical analysis was conducted under the conditions that the heating was concentrated at the center PHP only. Assuming a thermal bottleneck occurs at the center of a PHP configuration with stacked heating elements such as batteries, the amount of heating used here is similar to that in the uniform heating condition. In this case, PHPs 1 and 5 showed an increase in the evaporator temperature and thermal resistance. However, the PHP at the center, where the thermal bottleneck hot spot occurred, shows a decrease in the thermal resistance and evaporator temperature compared to the uniform heating conditions with the same amount of heat applied. Therefore, 3D PHPs can mitigate the central thermal bottleneck.

Acknowledgments

This study was supported by the National Research Foundation of Korea (NRF) funded by the Korean government (MSIT) [NRF-2021R1I1A3047845, NRF-2022R1A4A3023960].

Nomenclature

ρ	: Density
ρ_v	: Vapor density
ρ_l	: Liquid density
$\overrightarrow{v_v}$	: Vapor velocity
$\overrightarrow{v_l}$	: Liquid velocity
α_v	: Vapor volume fraction
α_l	: Liquid volume fraction
m_{vl}	: Mass transfer from vapor to liquid
m_{lv}	: Mass transfer from liquid to vapor
β_e	: Evaporation time relaxation coefficient
β_c	: Condensation time relaxation coefficient
T_{sat}	: Saturation temperature
T_v	: Vapor phase temperature

T_l : Liquid phase temperature
μ : Viscosity
μ_v : Vapor viscosity
μ_l : Liquid viscosity
E : Internal energy
$\vec{F}$: Body force
$\vec{g}$: Gravitational acceleration
k_{eff} : Effective thermal conductivity
S_h : Energy source term
p : Pressure
R : Gas constant
R_{th} : Thermal resistance
T_e : Evaporator temperature
T_c : Condenser temperature
Q_{input} : Heat flow rate

References

[1] D. T. Vo, H. T. Kim, J. H. Ko and K. H. Bang, An experiment and three-dimensional numerical simulation of pulsating heat pipes, *Int. J. Heat Mass Transf.*, 150 (2020) 119317.

[2] H. Akachi, *Structure of a Heat Pipe*, US Patent, US4921041A (1990).

[3] Y. J. Youn and S. J. Kim, Fabrication and evaluation of a slicon-based micro pulsating heat spreader, *Sens. Actuator A-Phys.*, 174 (2012) 189-197.

[4] D. S. Jang, J. S. Lee, J. H. Ahn, D. Kim and Y. Kim, Flow patterns and heat transfer characteristics of flat plate pulsating heat pipes with various asymmetric and aspect ratios of the channels, *Appl. Therm. Eng.*, 114 (2017) 211-220.

[5] V. M. Patel, Gaurav and H. B. Mehta, Influence of working fluids on startup mechanism and thermal performance of a closed loop pulsating heat pipe, *Appl. Therm. Eng.,* 110 (2017) 1568-1577.

[6] P. Charoensawan, S. Khandekar, M. Groll and P. Terdtoon, Closed loop pulsating heat pipes part A: parametric experimental investigations, *Appl. Therm. Eng.,* 23 (2003) 2009-2020.

[7] H. Han, X. Cui, Y. Zhu and S. Sun, A comparative study of the behavior of working fluids and their properties on the performance of pulsating heat pipes (PHP), *Int. J. Therm. Sci.,* 82 (2014) 138-147.

[8] V. K. Karthikeyan, K. Ramachandran, B. C. Pillai and A. B. Solomon, Effect of nanofluids on thermal performance of closed loop pulsating heat pipe, *Exp. Therm. Fluid Sci.,* 54 (2014) 171-178.

[9] M. Zufar, P. Gunnasegaran, H. M. Kumar and K. C. Ng, Numerical and experimental investigations of hybrid nanofluids on pulsating heat pipe performance, *Int. J. Heat Mass Transf.*, 146 (2020) 118887.

[10] D. S. Jang, E. Lee, S. H. Lee and Y. Kim, Thermal performance of flat plate pulsating heat pipes with mini- and microchannels, *Int. J. Air-Cond. Refrig.*, 22 (4) (2014) 1-7.

[11] K. Chien, Y. Lin, Y. Chen, K. Yang and C. Wang, A novel design of pulsating heat pipe with fewer turns applicable to all orientations, *Int. J. Heat Mass Transf.*, 55 (2012) 5722-5728.

[12] D. S. Jang, H. J. Chung, Y. Jeon and Y. Kim, Thermal performance characteristics of a pulsating heat pipe at various non-uniform heating conditions, *Int. J. Heat Mass Transf.*, 126 (B) (2018) 855-863.

[13] Z. Kang, D. Shou and J. Fan, Numerical study of a novel Single-loop pulsating heat pipe with separating walls within the flow channel, *Appl. Therm. Eng*., 196 (2021) 117246.

[14] J. Wang, Y. Pan and X. Liu, Investigation on start-up and thermal performance of the single-loop pulsating heat pipe with variable diameter, *Int. J. Heat Mass Transf.,* 180 (2021) 121811.

[15] J. Wang, J. Xie and X. Liu, Investigation on the performance of closed-loop pulsating heat pipe with surfactant, *Appl. Therm. Eng.*, 160 (2019) 113998.

[16] J. Wang, J. Xie and X. Liu, Investigation of wettability on performance of pulsating heat pipe, *Int. J. Heat Mass Transf.,* 150 (2020) 119354.

[17] Y. Han, Y. Kwon, W. S. Kim and Y. H. Na, Experimental study on oscillating heat pipe with three-dimensional structure, *Trans. Korean Soc. Mech. Eng. B*, 42 (12) (2018) 769-775.

[18] L. Chu, Y. Ji, Z. Liu, C. Yu, Z. Wu, Z. Wang, Y. Yang and X. Yang, Structure optimization of a three-dimensional coil oscillating heat pipe, *Int. J. Heat Mass Transf.*, 183 (C) (2022) 122229.

[19] J. Qu, J. Zhao and Z. Rao, Experimental investigation on the thermal performance of three-dimensional oscillating heat pipe, *Int. J. Heat Mass Transf.,* 109 (2017) 589-600.

[20] Ansys Inc.*, ANSY FLUENT Theory Guide*, Release 15, Ansys Inc. (2013).

[21] W. H. Lee and R. W. Lyczkowski, The basic character of five two-phase flow model equation sets, *Int. J. Numer. Meth. Fluids.,* 33 (2000) 1075-1098.

[22] N. Saha, P. K. Das and P. K. Sharma, Influence of process variables on the hydrodynamics and performance of a single loop pulsating heat pipe, *Int. J. Heat Mass Transf*., 74 (2014) 238-250.

Jongmin Jung is a M.S. student of Department of Refrigeration Engineering at Korea Maritime and Ocean University, Busan, Korea. He received his B.S degree in refrigeration engineering from Chonnam National University in Korea in 2021.

Yongseok Jeon is an Associate Professor in the Department of Mechanical Engineering at Korea Maritime and Ocean University, Busan, Korea. He received B.S. and the Ph.D. degrees in Mechanical Engineering from Korea University, Seoul, Korea. His research interests include thermal engineering, heat transfer, and energy system.